



# Deformation of Subway Tunnels Affected by Adjacent Excavation: In-situ Monitoring and Centrifugal Model Test

Jifei Cui<sup>1,2</sup>, Jingpei Li<sup>1,2</sup>(✉), Lin Li<sup>1,2</sup>, and Gaowen Zhao<sup>1,2</sup>

<sup>1</sup> Key Laboratory of Geotechnical and Underground Engineering of Ministry of Education, Tongji University, Shanghai 200092, China

lijp2773@tongji.edu.cn

<sup>2</sup> Department of Geotechnical Engineering, Tongji University, Shanghai 200092, China

**Abstract.** The basement excavation will change the initial stress equilibrium of the surrounding soil and hence result in surface subsidence and strata movement. The adjacent subway tunnels would be inevitably influenced by the basement excavation in the dense urban environment. Based on the excavation engineering of Wufangyuan project in Shanghai, the effects of excavation on adjacent subway tunnels are studied by monitoring data and centrifugal model test in this paper. Detailed discussions are performed to investigate the different excavation partitions and excavation sequences. The deformations of an adjacent tunnel under different construction conditions are obtained and the comparisons between the tests are conducted. The results indicate that the excavation of the soil in the areas closer to the tunnel induced greater additional settlements and additional convergence. Some of the construction technologies were employed to reduce the deformation of adjacent tunnels including setting a small partition in the foundation excavation close to the tunnel, excavating the small partition after the completion of the main body of foundation excavation as well as enhancing the support in the direction perpendicular to the tunnel

**Keywords:** Basement excavation · Adjacent subway tunnels  
Field monitoring · Centrifugal model test

## 1 Introduction

The rapid development of urban construction calls for growing excavation engineering in an urban area, and the metro system has been a lifeline of city transport. A lot of deep foundation pits are dug adjacent to existing tunnels. Effects on ground movement induced by deep excavations would cause a significant influence on the stress and the movement of tunnels (Wei et al. 2013). The structural cracks might lead to leakage and the rail differential displacements, which may seriously affect the safety of subway (Zhang et al. 2013a, b). Therefore, the deformations of the tunnel should be controlled within the acceptable level during excavation.

Lots of literature has reported the effects of deep excavations on the adjacent metro tunnel nearby. Zhang et al. (2013a, b) presented a semi-analytical method to evaluate

the heave of underlying tunnel induced by adjacent excavation and verified by field measurement results. Many previous studies (Dolezalova 2001; Sharma et al. 2001; Ge 2002; Hu et al. 2003; Zhang et al. 2007; Kog 2010) focus on numerical simulation approach. In their works, surrounding unloading soils and existing tunnels are modeled as a whole during the numerical discretization process. Birth and death element technology is used to simulate the soil excavation. Wei et al. (2014) analyzes the rules and characteristics of the vertical displacement, horizontal displacement, and convergence of the shield-driven tunnel at different construction stages based on the monitoring data. Zheng et al. (2010) study the influence of a basement excavation on an existing tunnel by carrying two centrifuge model tests.

In order to obtain a better understanding of the effects of foundation pit excavation on adjacent tunnels, the monitoring data of Wufangyuan project is analyzed in this study. Two centrifuge model tests were carried out to study the influence of excavation on an existing adjacent tunnel and the excavation scheme is compared and optimized.

## 2 Engineering General Situation

### 2.1 Site Condition

Shanghai is located near the front fringe of Yangtze River Delta in China. The Wufangyuan excavation is situated in Huangpu District, and the site plan is shown in Fig. 1. The area of the foundation pit is about 12 000 m<sup>2</sup>, and the depth is 9.2–9.65 m. The foundation pit is divided into three areas, and the excavation sequence is A, B, and C. The south side of the foundation pit is the Shanghai Rail Transit Line 9 which has been completed and operated. The distance between the tunnel and the foundation pit is 15–20 m and the buried depth of the top of the tunnel is about 10 m.

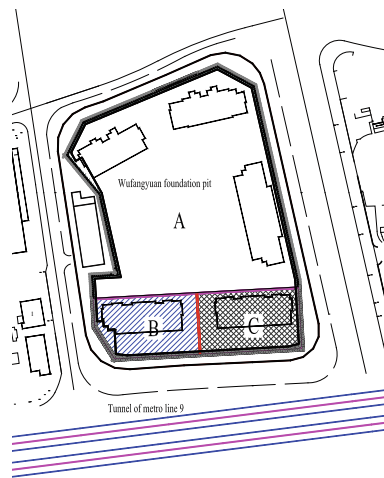


**Fig. 1.** Site plan of the Wufangyuan foundation pit

The retaining structure of district A is bored piles ( $\text{Ø}850@600$ ,  $L = 20.1$  m), while the retaining structures of districts B and C are concrete diaphragm walls with a thickness of 800 mm ( $L = 25$  m). The middle wall is concrete diaphragm wall with a thickness of 600 mm ( $L = 21.6$  m). Figure 2 shows a cross section of the support system of B and C district, which consist of concrete diaphragm wall, two concrete struts, piles and steel columns.

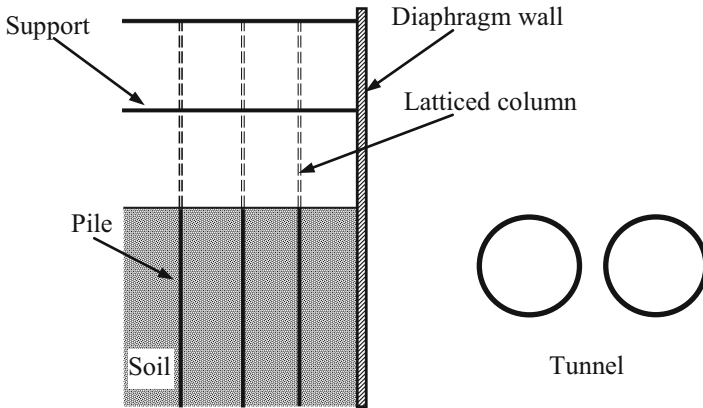


Fig. 2. Cross section of the retaining structure and tunnel

## 2.2 Geology

The strata of Shanghai are thick soft soils comprising Quaternary alluvial and marine deposits. A high water content, low shear strength, high compressibility and low ground bearing capacity are typical characteristics of the soft soil in Shanghai. Typical soil profiles from up to down obtained from site investigation are shown in Table 1. The groundwater conditions are approximately hydrostatic 1.0 m below ground level.

Table 1. Soil parameters

No.	Layer name	Thickness /m	Unit weight ( $\gamma$ )/ ( $\text{kN/m}^3$ )	Cohesion ( $c$ )/kPa	Internal friction angle ( $\varphi$ ) $^\circ$	Poisson ratio ( $\nu$ )
①	Miscellaneous fill	2.67	17.5	12	11	0.40
②	Silty clay	1.93	17.9	18	14	0.35
③	Muddy silty clay	5.1	17.4	12	17.5	0.41
④	Muddy clay	8.1	16.5	13	10.5	0.42
⑤ <sub>1</sub>	Clay	10.2	17.2	17	15	0.36
⑤ <sub>2</sub>	Silty clay	5.9	18.1	17	21.5	0.27

### 2.3 Construction Procedure of the Excavation

The foundation pit is divided into three areas named A, B and C. The excavation sequence is first A, then B, and finally C. The soil of each area is divided into three layers, and the excavation depth is 2 m, 4.5 m, 3.5 m respectively. Table 2 summaries the main construction stages of the excavation.

**Table 2.** Construction stages

Stage	Construction operation	Day
1	Excavation of the first layer in A district, construction of the first support	36
2	Excavation of the second layer in A district, construction of the second support	30
3	Excavation of the third layer in A district, construction of the Base Slab	57
4	Excavation of the first layer in B district, construction of the first support	32
5	Excavation of the second layer in B district, construction of the second support	30
6	Excavation of the third layer in B district, construction of the Base Slab	33
7	Excavation of the first layer in C district, construction of the first support	33
8	Excavation of the second layer in C district, construction of the second support	34
9	Excavation of the third layer in C district, construction of the Base Slab	37

## 3 Observed Tunnel Deflections

### 3.1 Additional Settlement

Along the tunnel paralleling to the edge of the foundation pit, 28 measuring points are arranged on the upper and lower tunnel segments, respectively, to monitor the settlement of the tunnels. Figure 3 shows the additional settlement of the tunnel induced by the excavation from stage 1 to stage 9.

Figure 3 shows that the construction of the pre-excavation stage, such as diaphragm wall construction and pile foundation construction, induce slight rise of the tunnel. With the continuous excavation of the soil, the vertical displacement of the tunnel has changed from rising at the beginning to sinking, then increasing gradually. This is mainly because of the soil settlement out of the pit caused by the excavation. As seen from Fig. 3, the tunnel settlement caused by excavation after the third step is obviously greater than before. It means that the excavation of the soil in B and C areas induced greater influence on tunnel settlement than area A, which is closer to the tunnel seen in Fig. 1. Comparing the settlement of the segment along the length of the tunnel, it can be seen that the settlement of the segment beyond the boundary of the foundation pit is much smaller than the settlement at the midpoint of the pit edge.

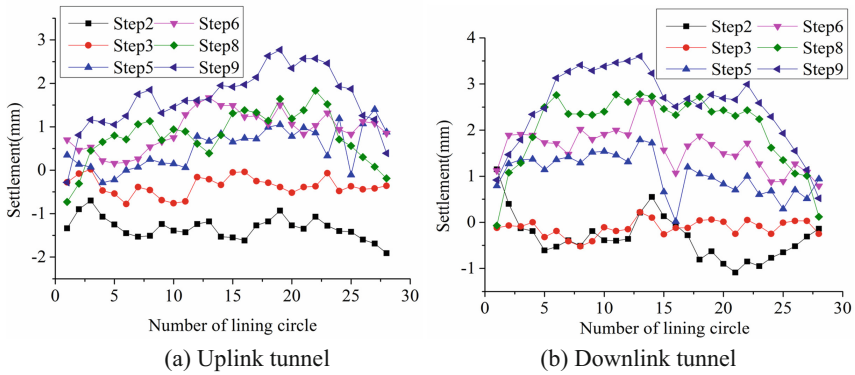


Fig. 3. Additional tunnel settlements induced by excavation

### 3.2 Additional Convergence

For determining additional convergence of the tunnel, the convergence was surveyed by 17 measuring points on the upper and lower tunnel segments, respectively. Four of these 34 measuring points are analyzed here for the additional convergence of the tunnel. Two of them named NO.1 and NO.4 are beyond the boundary of the foundation pit, and the other two measuring points named NO.2 and NO.3 are located at the tunnel corresponding to the midpoint of the boundary. Figure 4 shows the additional convergence of the four measuring points.

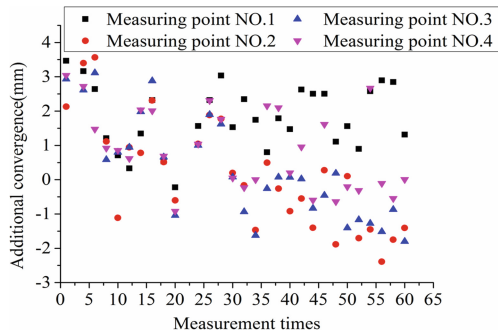


Fig. 4. Additional convergences induced by excavation

It can be seen from Fig. 4 that the additional convergence of measuring points NO.2 and NO.3 changed to the negative value which means that the excavation-induced inward compression of the tunnel. The additional convergence of the tunnel has been basically negative when the foundation pit is excavated in B and C areas. But the additional convergence of measuring points NO.1 and NO.4 vary near the averaged value and remain essentially unchanged. This shows that the excavation has a great impact on the tunnel within the foundation pit boundary, especially on the

tunnel near the middle of the edge, but has little influence on the tunnel out of the foundation pit boundary.

## 4 Centrifugal Model Test

### 4.1 Apparatus

The geotechnical centrifuge in the key laboratory of geotechnical and underground engineering, at Tongji University, is a 150 gt machine with 3 m platform radius able to achieve accelerations up to 200 g. It has an automatic in-flight balancing system and a data acquisition system. A swinging model platform is located at the end of the centrifuge arm and is the base where the model container will be fixed. The soil and foundation pit model was installed on the model container (Fig. 5), 900 mm long, 700 mm wide, and 700 mm height. One side of the model container was equipped with transparent organic glass through which the deformation of the soil could be observed.

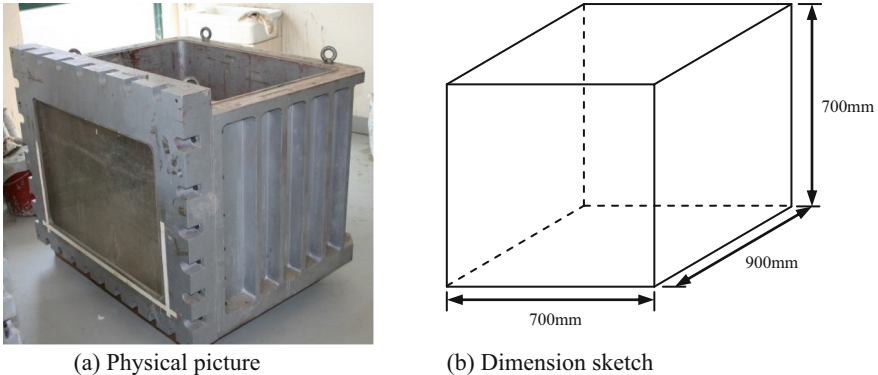
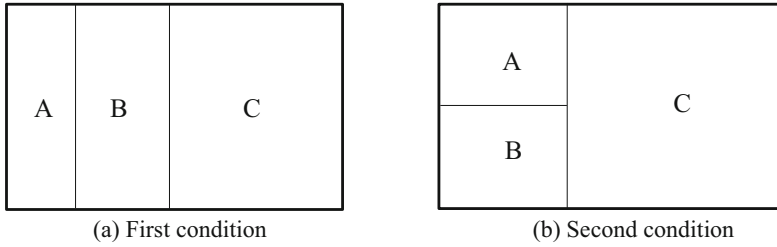


Fig. 5. Model container

### 4.2 Model

The centrifugal acceleration in this test is 100 g, which means the similarity ratio of this test is 1/100. There are two group of tests were conducted, one of which was in accordance with the excavation partitions and sequence of the Wufangyuan foundation pit. The second group is a parallel test with different excavation partitions and sequence of Wufangyuan foundation pit to study the impact on the tunnel of the excavation partitions and sequence, as shown in Fig. 6.

The soil used in the tests is a type of silty clay taken from ⑤<sub>2</sub> layer of Wufangyuan foundation pit. The soil parameter is shown in Table 1. Before the test, the soil obtained from the site was dehydrated and crushed, configured the same moisture content as the field, and placed in a vacuum mixer, consolidated on the centrifugal under acceleration of 100 g to recovery its original state.



**Fig. 6.** Excavation subarea

It is difficult to make a concrete foundation pit model and support system with a similar ratio of 1/100. Therefore, the aluminum alloy is used to simulate the retaining structure and support. The size of the model is calculated according to the similarity of the bending stiffness (retaining structure) and the compressive stiffness (support):

$$\left[ \frac{Et^3}{12(1-\nu^2)} \right]_{m1} = \left[ \frac{Et^3}{12(1-\nu^2)} \right]_{m2} \quad (1)$$

$$E_{m1}A_{m1} = E_{m2}A_{m2} \quad (2)$$

Where  $E$  is Elastic Modulus of retaining structure;  $t$  is thickness of diaphragm wall;  $\nu$  is Poisson ratio;  $m1$  representative prototype material and  $m2$  represents alternative materials.

The tunnel is simulated by PVC tube, and the size of the model is calculated by the similarity of longitudinal bending stiffness:

$$\eta \left[ \frac{E\pi(D^4 - d^4)}{64} \right]_{m1} = \left[ \frac{E\pi(D^4 - d^4)}{64} \right]_{m2} \quad (3)$$

where  $\eta$  is Longitudinal stiffness efficiency;  $E$  is Elastic Modulus of the tunnel;  $D$  is the outer diameter of the tunnel;  $d$  is the inner diameter of the tunnel;  $m1$  representative prototype material and  $m2$  represents alternative materials.

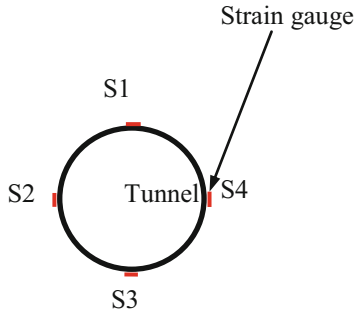
Four groups of strain gauges are pasted on the surface of the tunnel model to measure the deformation caused by excavation, as shown in Fig. 7.

### 4.3 Procedure

After completing the soil, the retaining structure and tunnel were installed and the model container was put into the centrifuge. The centrifuge runs for 5 min to simulate 35 days in actual operation after the foundation pit is excavated artificially. Table 3 summaries the main stages of the two tests and Fig. 8 shows the excavation process of the two tests.



(a) Physical picture



(b) Distribution of strain gauge on tunnel surface

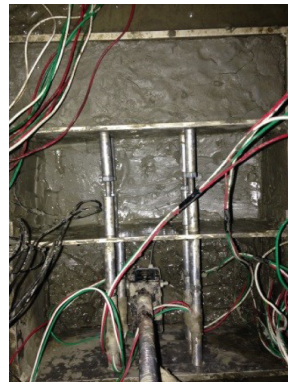
**Fig. 7.** Excavation subarea

**Table 3.** Test stages

Step	Construction operation	Time/min
1	First dewatering, excavate the first layer in A district, first support	5
2	Second dewatering, excavate the second layer in A district, second support	5
3	Third dewatering, excavate the third layer in A district	5
4	Excavate the first layer in B district, first support	5
5	Excavate the second layer in B district, second support	5
6	Excavate the third layer in B district	5
7	Excavate the first layer in C district, first support	5
8	Excavate the second layer in C district, second support	5
9	Excavate the third layer in C district	5



(a) First condition



(b) Second condition

**Fig. 8.** Excavation process



### 4.4 Results

The strain gauge data is recorded through the data acquisition system during the operation of the centrifuge. Figure 9 shows the additional strain of measuring points S1 and S2 on tunnel surface.

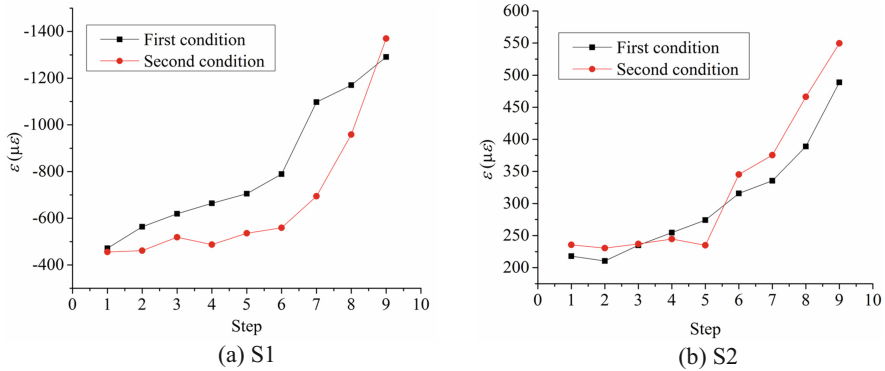


Fig. 9. Additional strain on tunnel surface induced by excavation

With the arrangement of strain gauge shown in Fig. 8, it is found that the excavation-induced downward and inward bending of the tunnel located at the side of the foundation pit, and this is consistent with the measured results shown in Fig. 3. The additional strain produced during the step 1–3 is very small, which means the excavation of district A in the far distance has little effect on the deformation of the tunnel. The additional strain of tunnel surface increases a certain extent during the excavation of district B and C. The blocked excavation can effectively control the tunnel deformation caused by excavation. The first condition can effectively restrain the deformation of the tunnel by the further partition of the districts C and add the diaphragm wall in the vertical direction, which shows that the excavation scheme adopted in the actual project is reasonable. Since the actual tunnel is joined by discontinuous segments, the dislocation between the segments should be noticed.

### 5 Conclusions

The field measured values of additional settlements and additional convergence induced by excavation were analyzed and two sets of centrifugal model tests were conducted to simulate the excavation near the subway tunnel. The following conclusions are drawn:

- (1) The excavation of the soil in the areas closer to the tunnel induced greater additional settlements and additional convergence of the tunnel. The additional settlements and convergence value of the segment beyond the boundary of the foundation pit is much smaller than the settlement at the midpoint of the pit edge.

- (2) The excavation induced downward and inward bending of the tunnel located at the side of the foundation pit. The blocked excavation can effectively control the tunnel deformation.
- (3) Further partition of the district near the tunnel and using the diaphragm wall in the vertical direction can significantly reduce the influence of excavation on adjacent tunnels.

## References

- Wei, S., Liao, S., Zhu, Y., Li, X.: Parametric study on the effect of deep excavation on the adjacent metro station in Suzhou. In: International Conference on Geotechnical and Earthquake Engineering, pp. 223–230 (2013)
- Zhang, J.F., Chen, J.J., Wang, J.H., Zhu, Y.F.: Prediction of tunnel displacement induced by adjacent excavation in soft soil. *Tunn. Undergr. Sp. Technol.* **36**(2), 24–33 (2013a)
- Zhang, Z.G., Huang, M.S., Wang, W.D.: Evaluation of deformation response for adjacent tunnels due to soil unloading in excavation engineering. *Tunn. Undergr. Space. Technol.* **38**, 244–253 (2013b)
- Dolezalova, M.: Tunnel complex unloaded by a deep excavation. *Comput. Geotech.* **28**(3), 469–493 (2001)
- Sharma, J.S., Hefny, A.M., Zhao, J., Chan, C.W.: Effect of large excavation on deformation of adjacent MRT tunnels. *Tunn. Undergr. Space. Technol.* **16**(2), 93–98 (2001)
- Ge, X.W.: Response of a shield-driven tunnel to deep excavations in soft clay. Doctor of Engineering thesis, Hong Kong University of Science and Technology, China (2002)
- Hu, Z.F., Yue, Z.Q., Zhou, J., Tham, L.G.: Design and construction of a deep excavation in soft soils adjacent to the Shanghai metro tunnels. *Can. Geotech. J.* **40**(5), 933–948 (2003)
- Zhang, Z.G., Zhang, X.D., Wang, W.D.: Numerical modeling analysis on deformation effect of metro tunnels due to adjacent excavation of foundation pit. *J. Wuhan Univ. Technol.* **29**(11), 93–97 (2007). (in Chinese)
- Kog, Y.C.: Buried pipeline response to braced excavation movements. *ASCE J. Perform. Constr. Facl.* **24**(3), 235–241 (2010)
- Wei, G., Li, G., Su, Q.: Analysis of the influence of foundation pit construction on an operating metro tunnel based on field measurement. *Mod. Tunn. Technol.* **51**(1), 179–185 (2014). (in Chinese)
- Zheng, G., Wei, S., Peng, S., Diao, Y., Ng, C.W.: Centrifuge modeling of the influence of basement excavation on existing tunnels. In: *Physical Modelling in Geotechnics, Two Volume Set* (2010)